Optical phonons of $Ca_{1.8}Sr_{0.2}CuO_3$ with the Cu-O chain structure

M. Yoshida, S. Tajima, N. Koshizuka, and S. Tanaka
Superconductivity Research Laboratory, International Superconductivity Technology Center, 1-10-13, Shinonome, Koto-ku, Tokyo 135, Japan

S. Uchida and S. Ishibashi
Department of Applied Physics, Faculty of Engineering, University of Tokyo, Bunkyo-ku, Tokyo 113, Japan
(Received 1 May 1991)

Raman and ir spectra of $Ca_{1.8}Sr_{0.2}CuO_3$ with the Cu-O chain structure have been investigated. Scattering peaks due to Raman-allowed A_g-mode phonons have been observed at 306 and 530 cm^{-1} at room temperature for the polarization of light along the *a* and *c* axes. On the other hand, when the polarization is along the *b* axis (chain direction), Raman-forbidden peaks have been observed at 235, 440, 500, and 690 cm^{-1} with strong second-order features, which show strong resonance enhancement at the charge-transfer gap energy of 2.0 eV. They are ascribed to the zone-boundary phonons, which appear through the strong coupling of the electron-hole pair excited on the Cu-O chain with phonons associated with the motion of atoms in the chain.

I. INTRODUCTION

The electronic structure and electron-phonon interaction associated with the Cu-O_2 plane structure have attracted much interest since the discovery of superconductivity in $(La,Sr)_2CuO_4$. Weber has shown that superconductivity up to 40 K of $(La,Sr)_2CuO_4$ can be explained by the strong coupling of holes with breathing-type lattice vibrations.[1] On the other hand, the importance of the long-range term in the electron-phonon interaction has been pointed out by Cohen, Pickett, and Krakauer[2] and Zeyher[3] to explain the superconductivity as high as 90 K of $YBa_2Cu_3O_7$.

Raman spectra of cuprates have been investigated intensively to clarify the role of phonons in superconductivity. In the spectra of La_2CuO_4, a series of normally forbidden peaks with strong second-order features have been observed when the incident and scattered electric vectors are in the Cu-O_2 plane.[4–7] Weber *et al.*[5] and Sugai[6] assigned those peaks to *X*-point phonons which appear through strong electron-phonon coupling with breathing-type vibrations. On the other hand, Zeiger *et al.*[7] proposed a model based on the excitation of the spin wave.

In the present study, we have investigated Raman and ir spectra of $Ca_{1.8}Sr_{0.2}CuO_3$ with Cu-O chain structure. Figure 1 shows crystal structures of Ca_2CuO_3 and La_2CuO_4. In Ca_2CuO_3 there is a chain of Cu—O bonds along the *b* axis, but no oxygen atom is located between Cu atoms neighboring along the *a* axis, being different from the Cu-O_2 plane structure of La_2CuO_4. We have observed a series of Raman-forbidden peaks in the scattering spectra of $Ca_{1.8}Sr_{0.2}CuO_3$ similar to that observed in La_2CuO_4. The Raman shifts of these peaks did not agree with zone-center TO-phonon energies and are ascribed to zone-boundary phonons, which appear through the strong coupling of the electron-hole pair excited on the Cu-O chain with the lattice vibrations associated with the chain.

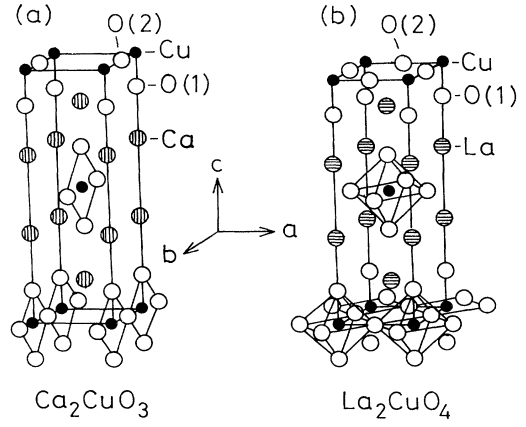

FIG. 1. Crystal structures of Ca_2CuO_3 and La_2CuO_4.

II. EXPERIMENT

Single crystals of $Ca_{1.8}Sr_{0.2}CuO_3$ were obtained using the flux method. Powders of Bi_2O_3, $SrCO_3$, $CaCO_3$, and CuO were mixed with a cation ratio of [Bi]:[Sr]:[Ca]:[Cu]=1:1:1:1. They were placed in alumina crucibles and heated to 1100 °C in air, cooled down to 950 °C at the rate of 5 °C/min, and then cooled gradually to 700 °C at the rate of 3.5 °C/h.

A schematic figure of the crystal used in the present study is shown in Fig. 2. The dimension of the crystal along the *b* axis is about 5 mm, but is less than 1 mm along the *a* and *c* axes. the orientation of the crystal was determined using the x-ray Laue method. The composition of metals were determined by the energy-dispersive

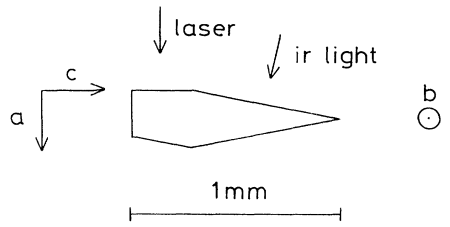

FIG. 2. Schematic figure of the sample used in the present study.

x-ray (EDX) spectroscopy. No contamination of Al or Bi was detected by the EDX method.

Raman spectra were measured in the backscattering configuration using both an Ar laser and a He-Ne laser as exciting light sources. The incident beam was focused on the *ab* or *bc* surfaces of the sample with a diameter of about 0.1 mm. The laser power was around 50 mW. The scattered light was detected with a Jobin Yvon U-1000 double monochromator and a photon-counting detection system with a Hamamatsu R-943 photomultiplier. Spectra were corrected for the wavelength dependence of the sensitivity of the detection system. In addition, spectra were corrected for the differences between the beam sizes of the Ar and He-Ne lasers, which was monitored using the 1330-cm^{-1} Raman peak of a diamond crystal.

Infrared reflection spectra were observed using a Bruker 113V spectrometer. Reflection spectra were measured using the inclined surface shown in Fig. 2 because we could not concentrate incident light on the *ab* or *bc* surfaces with a width below 0.3 mm.

III. RESULTS

A. Raman-scattering spectra

Figure 3 shows Raman-scattering spectra of $Ca_{1.8}Sr_{0.2}CuO_3$ measured at room temperature using 4880 Å light from an Ar laser. Spectra were taken with polarization of the incident and scattered light along the X, Y, and Z directions, where X, Y, and Z refer to the directions along the crystallographic a, b, and c axes, respectively. Spectra for (Y,Y) and (Z,Z) configurations were taken using the *bc* surface and that for (X,X) was taken using the *ab* surface of the sample.

In the (X,X) and (Z,Z) spectra, peaks are observed at 306 and 530 cm^{-1}. The 530-cm^{-1} peak is strong in the (Z,Z), but is weak in the (X,X). On the other hand, the (Y,Y) spectrum shows numerous broad lines extending to higher energies. The 306-cm^{-1} peak is also seen in the (Y,Y) configuration as well as (X,X) and (Z,Z) configurations, but the 530-cm^{-1} peak is not seen in this configuration. In the (Y,Z) configuration, no peak was seen (not shown).

In the three configurations shown in Fig. 3, scattering due to A_g-mode phonons is allowed (symmetry analysis will be given in Sec. IV A). In the spectra for (X,X) and (Z,Z) configurations, two peaks are observed which can be ascribed to the A_g-mode phonons. On the other hand, features observed in the (Y,Y) configuration cannot be explained by simple group-theoretical considerations.

The large anisotropy in the Raman spectra may be caused by the highly anisotropic optical properties of this material. In the optical-absorption measurements by Tokura *et al.*,[8] an absorption peak has been observed at 2.0 eV for the Y-polarized light and ascribed to the charge-transfer (CT) excitation associated with the Cu-O chain. Figure 4 shows the Raman spectrum of $Ca_{1.8}Sr_{0.2}CuO_3$ for the (Y,Y) configuration observed using a 6328 Å (1.96 eV) light from a He-Ne laser. The inset shows the absorption spectrum measured by Tokura *et al.*[8] Strong enhancement of the scattering peaks are seen when the excitation energy changes from 2.54 eV (4880 Å) to 1.96 eV (6328 Å) (note the difference of the scales of the ordinates in Figs. 3 and 4). Among the ob-

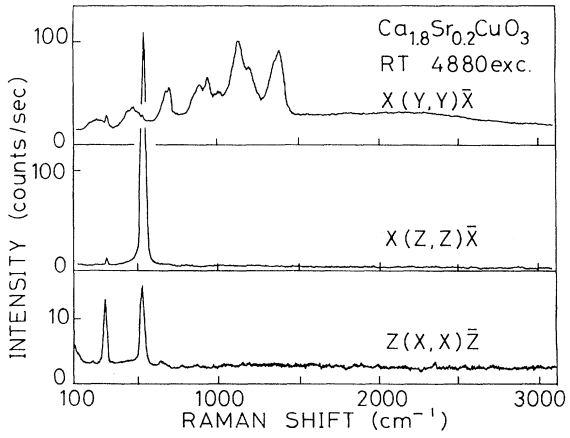

FIG. 3. Raman-scattering spectra of $Ca_{1.8}Sr_{0.2}CuO_3$ measured at room temperature using 4880 Å light from an Ar laser.

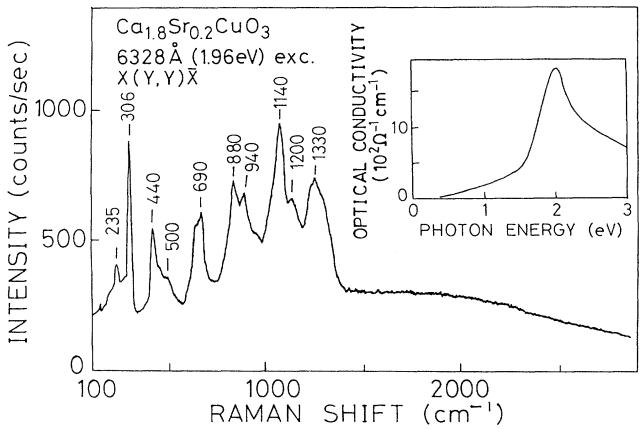

FIG. 4. Raman-scattering spectra of $Ca_{1.8}Sr_{0.2}CuO_3$ measured at room temperature using a 6328 Å (1.96 eV) light from a He-Ne laser for the (Y,Y) configuration. The inset shows the absorption spectra for the polarization parallel to the Y direction measured by Tokura *et al.* (see Ref. 8).

served peaks, the peaks below 500 cm^{-1} show stronger enhancement than the peaks above 500 cm^{-1}. This is probably because the scattered photon energies of peaks with smaller Raman shifts are closer to the CT-gap energy when excited at 1.96 eV. A broad peak at around 250 cm^{-1} in Fig. 3 turns into a sharp peak at 235 cm^{-1}, and a broad feature at around 480 cm^{-1} in Fig. 3 separates into a peak at 440 cm^{-1} and a shoulder at 500 cm^{-1} in Fig. 4.

It should be noted that, in this spectrum, peaks at 880, 940, 1140, 1200, and 1330 cm^{-1} can be explained as the combinations of the 440-, 500-, and 690-cm^{-1} peaks as, e.g., the 880-cm^{-1} peak is due to two-phonon scattering of the 440-cm^{-1} phonon, the 940-cm^{-1} peak due to the combination of the 440- and 500-cm^{-1} phonons, and so on. In addition to them, a broad structure is observed at around 2000 cm^{-1}. This structure is observed when excited at 2.54 eV (see Fig. 3) as well as at 1.96 eV and is also a Raman-scattering peak rather than a luminescence peak.

B. Infrared spectra

In the previous section, it has been shown that Raman-forbidden peaks appear when the electric-field vectors of the incident and scattered lights are along the Cu-O chain direction. In order to clarify the origins of these peaks, we have measured infrared reflection spectra. Figures 5(a) and 5(b) show reflection spectra of $Ca_{1.8}Sr_{0.2}CuO_3$ at room temperature for electric-field vectors $\mathbf{E}\|b$ and $\mathbf{E}\perp b$, respectively. In Fig. 5(a) structures due to three B_{2u} phonons are clearly seen. The solid curve is the fit to the experimental results (solid circles) using the oscillator model. By this fitting we have obtained TO- (LO-) phonon energies as 215 (260), 340 (430), and 660 (700) cm^{-1}.

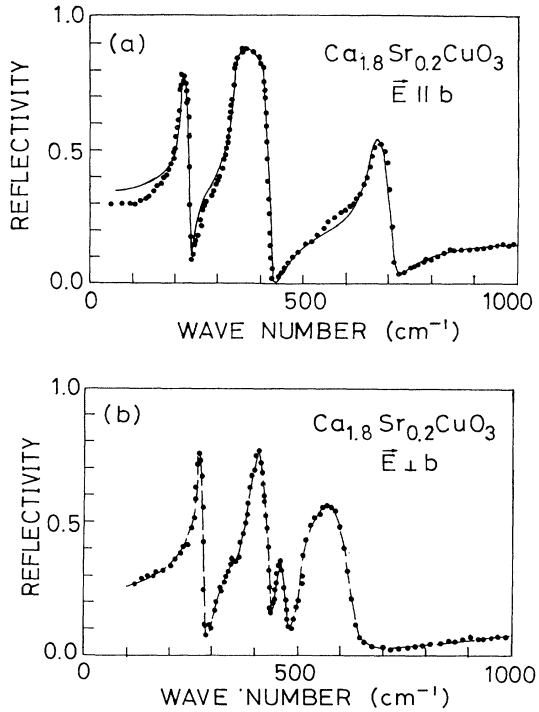

FIG. 5. Infrared reflection spectra of $Ca_{1.8}Sr_{0.2}CuO_3$ at room temperature for polarization of light (a) $\mathbf{E}\|b$ and (b) $\mathbf{E}\perp b$. The solid curve in (a) is the calculation curve based on the oscillator model in which the dielectric constant is defined as $\varepsilon(\omega)=\varepsilon_\infty[1+\sum_j(w_{\mathrm{LO}j}^2-w_{\mathrm{TO}j}^2)/(w_{\mathrm{TO}j}^2-w^2-iw\gamma_j)]$. The dashed curve in (b) is a guide to the eye.

In Fig. 5(b) structures due to B_{1u} and B_{3u} phonons are seen. A quantitative analysis of this spectrum using the oscillator model could not be performed since two components corresponding to $\mathbf{E}\|a$ and $\mathbf{E}\|c$ are mixed in this spectrum. However, we can roughly estimate the TO- and LO-phonon energies from the positions of peaks and dips of the spectrum. The obtained TO- (LO-) phonon energies are 260 (290), 410 (430), 460 (480), and 580 (630) cm^{-1}. In addition to them, weak structures are seen at around 350 and 540 cm^{-1}, which may also be caused by phonons.

It should be noted that the three Raman-forbidden peaks 690, 500, 440 cm^{-1} nearly agree with the LO-phonon energies 700 (B_{2u} symmetry), 480, and 430 cm^{-1} (B_{1u} or B_{3u} symmetries), but are a little larger than the TO-phonon energies.

IV. DISCUSSION

A. Symmetry analysis

The Ca_2CuO_3-type crystal has an orthorhombic structure with space group D_{2h}^{25} ($Immm$). The reduced representations of optical phonons at the Γ point are

$$\Gamma=2A_g+2B_{2g}+2B_{3g}+3B_{1u}+3B_{2u}+3B_{3u}\ .$$

The A_g-mode phonons are composed of the displacements of Ca and O(1) along the c axis as shown in Fig. 6 and the B_{2g} and B_{3g} modes along the a and b axes, respectively. Raman scattering due to A_g-mode phonons is allowed in the (X,X), (Y,Y), and (Z,Z) geometry. The B_{2g} and B_{3g} phonons are active in the (X,Z) and (Y,Z) geometries, respectively.

The B_{1u}, B_{2u}, and B_{3u} phonons are composed of the displacements of O(1), O(2), Ca, and Cu along the c, b, and a axes, respectively, and are ir active for the polarization along each direction.

B. Identification of the ir-active phonons

In Sec. III B, B_{2u}-phonon energies have been determined as 215, 340, and 660 cm^{-1}. Since the vibration modes associated with oxygen atoms are expected to have larger energies than those of metal atoms, we can associate the 340- and 660-cm^{-1} phonons to the vibration of oxygens. The B_{2u}-mode vibration of the O(2) atom is of the stretching type where the bond length between Cu and O changes, while that of O(1) is of the bending type where the length does not change. Since stretching-mode phonons are expected to have energies larger than the bending-mode ones, the 660-cm^{-1} phonon can be ascribed to the stretching vibration of O(2) and the 340-cm^{-1} phonon to the bending vibration of O(1). The 215-cm^{-1} phonon can be assigned to the vibrational mode

where the Ca atom displaces in the opposite direction to the other atoms (see Fig. 6).

In Fig. 5(b) structures due to the B_{1u} and B_{3u} phonons have been observed. Among them, the highest-energy phonon at 580 cm^{-1} can be assigned as the stretching vibration of O(1) along the c axis (B_{1u}). The 410-, 460-, and 540-cm^{-1} phonons are tentatively assigned to the bending vibrations of O(1) (B_{3u}) or O(2) (B_{1u} or B_{3u}), while the 260- and 350-cm^{-1} phonons may be related to the vibrations of Ca and/or Cu atoms.

C. Identification of the Raman peaks

1. *Raman-allowed peaks*

Several peaks have been observed in the Raman spectra of $Ca_{1.8}Sr_{0.2}CuO_3$ as shown in Sec. III A. Two sharp peaks have been observed at 306 and 530 cm^{-1} for (X,X) and (Z,Z) geometries (Fig. 3). Since two A_g-mode phonons are allowed in these configurations, we can assign them to A_g-mode phonons. The 530-cm^{-1} peak can be assigned as the vibration of O(1) and the 306-cm^{-1} peak as the vibration of Ca (Fig. 6).

Scattering due to the 530-cm^{-1} peak is strong in the (Z,Z) but is weak in the (X,X) and (Y,Y) configurations. This polarization dependence can be explained by taking into account the anisotropic electronic structures as follows. The highest occupied states of $Ca_{1.8}Sr_{0.2}CuO_3$ are expected to be composed of the antibonding Cu—O bond as in the superconducting cuprates.[9] Then optical transition is expected to occur, for the Z-polarized light, between the $2p_z$ state of O(1) and $4s$ or $3d$ states of Cu. This transition is forbidden for the X- or Y-polarized lights. Holes created on the O(1) atom are expected to couple strongly with the vibrations of the same atom.

2. *Raman-forbidden peaks*

Before discussing the origin of the Raman-forbidden peaks of $Ca_{1.8}Sr_{0.2}CuO_3$, we want to point out the resemblance of them to those of La_2CuO_4. Figure 7 shows the Raman spectrum of La_2CuO_4 measured at room temperature for the (X,X) configuration.[10] Peaks have been observed at 220, 300, 470, 530, 710, 920, 1210, and 1420 cm^{-1}, where the peaks above 920 cm^{-1} can be explained as combinations of the 470-, 530-, and 710-cm^{-1} peaks as was pointed out in Refs. 4–6. The 220-cm^{-1} peak is due to the Raman-allowed A_{1g}-mode phonon, but the 300-, 470-, 530-, and 710-cm^{-1} peaks cannot be explained by a simple group-theoretical consideration.[5,6]

Infrared spectra of La_2CuO_4 have been measured by several groups.[11] The TO- (LO-) phonon energies associated with oxygen in the Cu-O_2 plane have been determined as 354 (466) (A_{2u} mode in tetragonal crystal symmetry, where oxygen atoms move along the c direction), 359 (446) (E_u mode, where oxygen atoms move along the a direction), and 669 (694) cm^{-1} (E_u mode).[11] The Raman shifts 470, 530, and 710 cm^{-1} are close to the LO-phonon energies, but are a little larger than the TO-phonon energies.

In ionic crystals it has been found that scattering due to Raman-forbidden LO phonons occurs near resonance with fundamental electronic transitions, which is caused by an intrinsic bulk effect dependent on the finite **k** vector of light.[12] In order to investigate the dependence of the spectral features on the **k** vector of the incident and/or scattered light, we have measured scattering spectra using the *ab* surface as well as the *bc* surface. However, no change has been observed in these two cases. Thus scattering peaks observed in the present measurements cannot be ascribed to LO phonons.

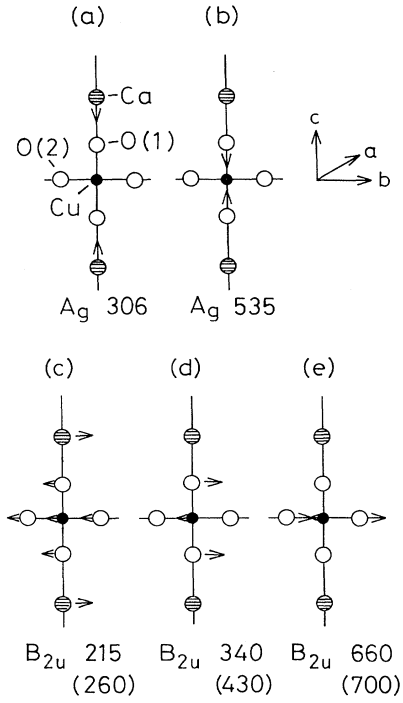

FIG. 6. Schematic figures of displacements of atoms in some zone-center lattice vibrations of Ca_2CuO_3.

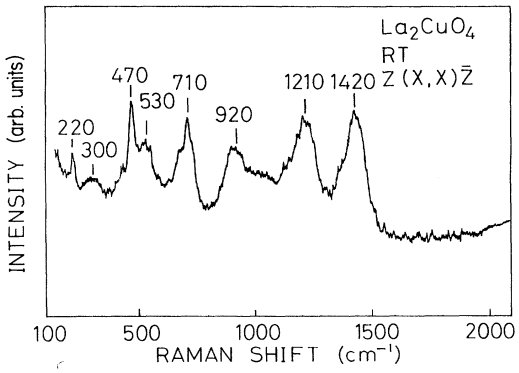

FIG. 7. Raman-scattering spectrum of La_2CuO_4 measured at room temperature using 5145 Å light from an Ar laser for the (X,X) configuration.

The Raman shifts do not agree with the zone-center TO-phonon energies. However, it may be possible that they are due to zone-boundary phonons. In La_2CuO_4 it is expected that electrons couple strongly with the planar breathing-type vibration of oxygen in the $Cu\text{-}O_2$ plane [phonons at the X point in the Brillouin zone with the $\mathbf{k}$ vector (0.5,0.5,0)].[1,12] The LAPW calculation by Cohen, Pickett, and Krakaur[13] has given the X-point breathing- and quadrupolar-type vibration energies of La_2CuO_4 as 725 and 475 cm^{-1}, respectively, which agree well with the 710- and 470-cm^{-1} Raman peaks (Fig. 7). A shell-model calculation by Mostoller *et al.*[11] gives the three highest phonon energies at the X point as about 720, 530, and 450 cm^{-1}, which also agree with the Raman shifts (displacements of atoms in each mode are not given in Ref. 11).

$Ca_{1.8}Sr_{0.2}CuO_3$ has a Cu-O chain different from the $Cu\text{-}O_2$ plane in La_2CuO_4. However, similar strong electron-phonon coupling is expected in $Ca_{1.8}Sr_{0.2}CuO_3$ between the electron-hole pair created through the Cu-O charge-transfer excitation and the axial breathing-type vibration of oxygen with the y component of the $\mathbf{k}$ vector, $k_y=0.5$. We can ascribe the 690-cm^{-1} peak of $Ca_{1.8}Sr_{0.2}CuO_3$ to the axial breathing vibration of O(2) with $k_y=0.5$. The 440- and 500-cm^{-1} peaks are also expected to be due to zone-boundary phonons since the combination peaks of them with the 690-cm^{-1} peak has been observed (in the two-phonon scattering process, the momentum-conservation rule is fulfilled by the combination of two phonons with momenta $\mathbf{k}$ and $-\mathbf{k}$). These phonons must be ascribed to the vibration of O(2) rather than O(1) since, in the (Y,Y) configuration, the electron-hole pairs are created on the Cu-O chain and couple with the lattice vibrations associated with the Cu-O chain.

In the Brillouin zone of the body-centered orthorhombic crystals, a high-symmetry point in the plane with $k_y=0.5$ is point T with $\mathbf{k}=(0.5,0.5,0)$. There are three vibration modes associated with the displacements of O(2) with full symmetry at point T as shown in Fig. 8, where the vibration mode shown in Fig. 8(a) is expected to be the largest energy one. Thus we can ascribe the 690-cm^{-1} peak to this vibration mode. The two-phonon scattering peak of the 690-cm^{-1} phonon locates at around 1330 cm^{-1} when excited at 1.96 eV (Fig. 4), while it is around 1380 cm^{-1} when excited at 2.54 eV (Fig. 3). This is probably caused by the dispersion of the breathing mode shown in Fig. 8(a) in the plane of $k_y=0.5$ in the Brillouin zone. We tentatively assign the 500-cm^{-1} peak as another axial breathing-type vibration shown in Fig. 8(b) and the 440-cm^{-1} peak to the bending-type vibration shown in Fig. 8(c).

In La_2CuO_4 it has been pointed out that the orthorhombic distortion doubles the volume of the unit cell, which folds back the X-point phonons to zone-center ones, thus Raman allowed.[5,6] Such an effect does not occur in $Ca_{1.8}Sr_{0.2}CuO_3$. However, in $Ca_{1.8}Sr_{0.2}CuO_3$ the partial substitution of Ca by Sr breaks the spatial symmetry, which may cause the zone-boundary modes to become Raman allowed. Anyhow, the fact that scattering due to the zone-boundary phonons associated with oxygen in the Cu—O bond is strong both in $Ca_{1.8}Sr_{0.2}CuO_3$ with the Cu—O chain and La_2CuO_4 with the $Cu\text{—}O_2$ plane suggests that strong coupling of these phonons with the electron-hole pair excited on the Cu—O bond is a characteristic feature of the Cu-O compounds. This strong electron-phonon coupling is supposed to have the same origin as that observed in the ir-active phonon spectra for various layered cuprates.[14]

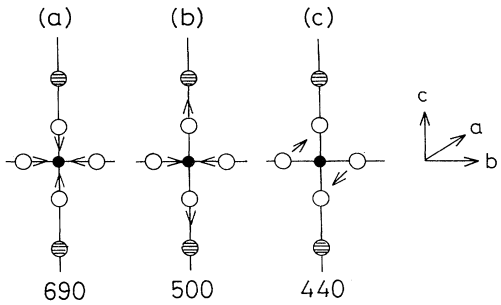

FIG. 8. Schematic figures of displacements of atoms in the three T-point lattice vibrations of Ca_2CuO_3.

In addition to the 690-, 500-, and 440-cm^{-1} peaks, a peak is seen at 235 cm^{-1} in the spectra of $Ca_{1.8}Sr_{0.2}CuO_3$. The 235-cm^{-1} peak can be ascribed to the vibration of Cu, though it is not clear whether this peak is due to zone-center or zone-boundary phonons. There are three vibration modes associated with the displacement of Cu along the three principal axes among which the B_{2u}-mode energy has been shown to be 215 cm^{-1} [Fig. 5(a)]. The broad width of the 235-cm^{-1} peak when excited at 2.54 eV (Fig. 3) may be caused by these three vibration modes.

Finally, we comment on the structure in the higher-energy region. As seen in Figs. 3 and 4, a broad peak is observed at around 2000 cm^{-1}. The origin of this structure is not clear. It may be caused by the higher-order ($n>3$) phonon scattering. Another possibility is magnon-pair scattering as observed in La_2CuO_4 around 3000 cm^{-1},[15] though magnetic order has not been confirmed in $Ca_{1.8}Sr_{0.2}CuO_3$.

V. SUMMARY

Raman-scattering spectra of $Ca_{1.8}Sr_{0.2}CuO_3$ were investigated using single crystals. When the polarization of light was perpendicular to the chain direction, peaks due to Raman-allowed A_g-mode phonons were observed. On the other hand, for the polarization along the chain direction, normally forbidden peaks were observed with strong second-order features. Strong resonance enhancement of these peaks at the CT-gap energy was observed when the sample was excited at 1.96 eV by a He-Ne laser. They were ascribed to the zone-boundary phonons with the motion of atoms associated with the chain. Similar spectra were obtained in La_2CuO_4 with the $Cu\text{-}O_2$ plane structure when the polarization is in the $Cu\text{-}O_2$ plane.

Thus the strong coupling of the electron-hole pairs excited on the Cu—O bond with the Cu-O vibrational-mode phonons was expected to be a characteristic feature of compounds with Cu—O bonds.

ACKNOWLEDGMENT

A part of this work was supported by the New Energy and Industrial Technology Development Organization.

[1]W. Weber, Phys. Rev. Lett. **58**, 1371 (1987).
[2]R. E. Cohen, W. E. Pickett, and H. Krakauer, Phys. Rev. Lett. **64**, 2575 (1990).
[3]R. Zeyher, Z. Phys. B **80**, 187 (1990).
[4]N. Koshizuka, H. Unoki, K. Oka, K. Hayashi, T. Okuda, and Y. Kimura, Jpn. J. Appl. Phys. **27**, L1300 (1988).
[5]W. H. Weber, C. R. Peters, B. M. Wanklyn, C. Chen, and B. E. Watts, Phys. Rev. B **38**, 917 (1988).
[6]S. Sugai, Phys. Rev. B **39**, 4306, (1989).
[7]H. J. Zeiger, A. J. Strauss, G. Dresselhaus, Y. C. Liu, P. J. Picone, and M. S. Dresselhaus, Phys. Rev. B **40**, 8891 (1989).
[8]Y. Tokura, S. Koshihara, T. Arima, H. Takagi, S. Ishibashi, T. Ido, and S. Uchida, Phys. Rev. B **41**, 11 657 (1990).
[9]L. F. Mattheiss, Phys. Rev. Lett. **58**, 1028 (1987). F. Hermann, R. V. Kasowski, and W. Y. Hsu, Phys. Rev. B **36**, 6904 (1987).
[10]The method of the crystal growth of La_2CuO_4 and results of the Raman measurements are planned to be published elsewhere.
[11]Experiments on the ir spectra of La_2CuO_4 are summarized in M. Mostoller, J. Zhang, A. M. Rao, and P. C. Eklund, Phys. Rev. B **41**, 6488 (1990).
[12]R. M. Martin and T. C. Damen, Phys. Rev. Lett. **26**, 86 (1971).
[13]R. E. Cohen, W. E. Pickett, and H. Krakauer, Phys. Rev. Lett. **62**, 831 (1989).
[14]S. Tajima, T. Ido, S. Ishibashi, T. Itoh, H. Eisaki, Y. Mizuo, T. Arima, H. Takagi, and S. Uchida, Phys. Rev. B **43**, 10496 (1991).
[15]K. B. Lyons, P. A. Fleury, J. P. Remeika, A. S. Cooper, and T. J. Negran, Phys. Rev. B **37**, 2353 (1988).